Contribution from the Department of Chemistry,
Iowa State University, Ames, Iowa 50011

Revision of the Structure of Zirconium Triiodide. The Presence of Metal Dimers

Abdessadek Lachgar, Douglas S. Dudis, and John D. Corbett*

Received October 25, 1989

Single-crystal X-ray studies on stoichiometric ZrI_3 by film and diffractometer means show that a considerable number of very weak diffraction intensities require an orthorhombic cell and space group *Pmmn* ($Z = 4$, $RuBr_3$-type), while the stronger ~75% of the reflection data are consistent with the hexagonal β-$TiCl_3$-type structure ($P6_3/mcm$, $Z = 2$) commonly assigned to many trihalides. (ZrI_3: $a = 12.594$ (6) Å, $b = 6.679$ (2) Å, $c = 7.292$ (2) Å; $R/R_w = 2.2/4.2\%$ for 741 reflections with $I/\sigma(I) > 3$, $2\theta \leq 70°$, Mo Kα radiation at 293 K.) The compound contains infinite chains of confacial (ZrI_6) octahedra that are distorted through pairing of the zirconium(III) atoms; d(Zr-Zr) = 3.172 (2) and 3.507 (2) Å. Data sets collected from the same crystal in the hexagonal setting were also refined in space groups $P6_3/mcm$ and $P\bar{6}2m$; the latter provides nominally satisfactory residuals but an incorrect result with less tightly bound dimers. A more complex structure (which we did not study) applies to the compound near the oxidized limit $ZrI_{3.4-3.5}$. Other structural and property studies on ZrI_3 and related phases are considered relative to these findings. A smaller pairing distortion in $ZrCl_3$ seems probable because of the less restrictive chlorine matrix. A second-order phase transition is possible between the $P6_3/mcm$ and *Pmmn* structures for these trihalides, and a continuous distortion from the equally spaced metal atoms of the former model can be expected, especially as a function of temperature.

Introduction

The trihalides of group 4 transition metals titanium, zirconium, and hafnium are all well-established compounds (except for the fluorides), and these occur in what has been, for the most part, described as a common structure variously identified as β-$TiCl_3$,[1] β-$ZrCl_3$,[2] ZrI_3,[3] or a variant TiI_3 (below).[4] (α-$TiCl_3$ and α-$TiBr_3$ exhibit a BiI_3-type structure, but the identification of α-$ZrCl_3$ in the same arrangement was in error.[5]) The same structure has also been reported for some trihalides of group 5 through group 8 transition metals. The structure is readily described as hexagonally closed-packed halides with metal atoms in one-third of the octahedral interstices, not in layers as in BiI_3 but centered in one-third of the semiinfinite strings of octahedral sites that run normal to the halogen layers. The structure thus contains chains of confacial trigonal antiprisms ("octahedra"), $^1_\infty[MX_{6/2}]$, that are held together only by dispersion forces, in accord with the very fibrous character usually noted for these crystals. There has been some dispute, however, whether this model is correct in detail regarding the regular spacing of the metal atoms along the chains.

The first published, comprehensive study of the structures of the three zirconium phases and of HfI_3 was by Dahl et al.[6] They found their Debye-Scherrer powder data were well described with the original[1] space group $P6_3/mcm$, which requires that the metal atoms in the chains be equally spaced. A similar result was reported shortly later for $ZrCl_3$ by Watts.[7] Single-crystal studies in support of these conclusions have more recently appeared for the three zirconium trihalides, all grown by an aluminum halide melt process.[8] Kleppinger et al.[9] saw no evidence of extra reflections for $ZrBr_3$ and refined their diffraction data well in the $P6_3/mcm$ space group. A particularly noteworthy result was the absence of any elongation of the thermal ellipsoids for the metal along the chain, or for the bromine atoms normal to the chain, that might be expected to signal the presence of other than equally spaced metal atoms ($R/R_w = 2.3/3.6\%$ for all data, $2\theta \leq 50°$, Mo Kα). Larsen, Wrazel, and Hoard[10,11] subsequently reported the refinement of single-crystal data for all three halides as well as for $ZrI_{3.4}$ in the same structure, although B_{22} values for all halide and B_{33} for metal in the iodides were all somewhat large. However, their results were somewhat more tentative, especially for the two heavier halides, because of three problems: diffuse extra electron density in the final ΔF maps, the observation of a few extra reflections, and somewhat larger refinement residuals. In the more relevant ZrI_3 case, these amounted to respectively 10-15% of a zirconium atom, a few unallowed $h0l$ reflections at 2-4% of F_o(max), and R/R_w values of 6.0/10.4% for data measured to $2\theta \leq 90°$ (Mo Kα).

Dahl et al.[6] noted from the beginning that this structure with equally spaced d^1 metal atoms should lead to a half-filled d_{z^2} band and metallic behavior (unless the band is particularly narrow). We have since observed that several properties seem inconsistent with this model; namely, all three zirconium halides are relatively poor semiconductors and exhibit weak paramagnetism.[12,13] In addition, the shared octahedra in their $ZrCl_3$ and $ZrBr_3$ models are actually elongated along the chains in spite of the short Zr-Zr distances (3.069, 3.152 Å, respectively) and presumed strong Zr-Zr bonding (bond orders = 0.56, 0.41).[14,15]

Some scattered powder pattern observations suggest the structure(s) for all three zirconium (and other) trihalides may be otherwise. Holze[4] observed the (001) reflection for all three phases, in violation of the systematic absences required for the $P6_3/mcm$ cell, and selected instead the subgroup $P\bar{6}2m$, which allows the metal atoms to pair. Struss and Corbett[16] discovered that HfI_3 exhibited 10 additional weak lines in its Debye-Scherrer pattern that could not be accounted for by a hexagonal cell unless a and b were doubled and c was quadrupled. They also found that this compound was significantly nonstoichiometric and more such lines appeared as the composition approached $HfI_{3.5}$. Significant nonstoichiometries pertain to the zirconium trihalides as well according to Daake and Corbett,[5] the compositions extending over the approximate ranges $ZrCl_{2.94(2)}$-$ZrCl_{3.03(2)}$ (at 440 °C), $ZrBr_{2.87(2)}$-$ZrBr_{3.23(2)}$ (435 °C), and $ZrI_{2.83(5)}$-$ZrI_{3.43(5)}$ (700/475 °C). Guinier powder patterns for the ideal compositions contained no violations of the systematic absences expected for $P6_3/mcm$, but the oxidized iodide exhibited seven extra reflections reminiscent of the behavior of the hafnium analogue. (We have subsequently seen extra lines in the pattern for ZrI_3 as well.)

Discrepancies were also observed years ago for other transition-metal halides that have customarily been assigned the ideal β-$TiCl_3$ structure. A large single crystal of TiI_3 was found to exhibit additional weak reflections, ~1% of the intensity of the major ones, that required doubling of the hexagonal a and b axes.[17]

(1) Natta G.; Corrandini, P.; Bassi, I. E.; Porri, L. *Atti. Accad. Naz. Lincei, Cl. Sci. Fis., Mat. Nat., Rend.* **1958**, *24*, 121.
(2) Adams, D. M. *Inorganic Solids*; J. Wiley: London, 1974; p 56.
(3) Wells, A. F. *Structural Inorganic Chemistry*, 5th ed.; Clarendon Press: Oxford, England 1984; p 419.
(4) Holze, E. Dissertation, Westfälische Wilhelms Universität, Münster, FRG, 1956.
(5) Daake, R. L.; Corbett, J. D. *Inorg. Chem.* **1978**, *17*, 1192.
(6) Dahl, L. F.; Chiang, T.-I.; Seabaugh, P. W.; Larsen, E. M. *Inorg. Chem.* **1964**, *3*, 1236.
(7) Watts, J. A. *Inorg. Chem.* **1966**, *5*, 281.
(8) Larsen, E. M.; Moyer, J. W.; Gil-Arnao, F.; Camp, M. J. *Inorg. Chem.* **1974**, *13*, 574.
(9) Kleppinger, J.; Calabrese, J. C.; Larsen, E. M. *Inorg. Chem.* **1975**, *14*, 3128.
(10) Larsen, E. M.; Wrazel, J. S.; Hoard, L. G. *Inorg. Chem.* **1982**, *21*, 2619.
(11) Wrazel, J. S. Ph.D. Thesis, University of Wisconsin, 1979.
(12) Clemmer, R. G. Ph.D. Thesis, University of Wisconsin; *Diss. Abst. B* **1977**, *38*, 674.
(13) Feldmann, C. D. Ph.D. Thesis, University of Wisconsin, 1979; *Diss. Abst. B* **1980**, *40*, 5661.
(14) Corbett, J. D. *Adv. Chem. Ser.* **1980**, *No. 186*, 329.
(15) Corbett, J. D. *Inorg. Chem.* **1983**, *22*, 2669.
(16) Struss, A. W.; Corbett, J. D. *Inorg. Chem.* **1969**, *8*, 227.
(17) von Schnering, H.-G. *Naturwissenschaften* **1966**, *53*, 359.

0020-1669/90/1329-2242$02.50/0

The same had been reported for $MoBr_3$,[18] and similar but evidently stronger extra reflections can also be seen for NbI_3.[19] Systematic absences for $MoBr_3$ and TiI_3 were consistent with the space group $P6_322$, which does not allow metal pairing. Unusually low magnetic susceptibilities generally observed for the entire group of trihalides in this structure have been attributed to strong metal–metal bonding.[17,20]

A resolution of these problems appeared to us to lie with either the refinement of good single-crystal data in the hexagonal space group $P\bar{6}2m$ suggested by Holze[4] or consideration of other lower symmetry cells. A hint of a solution for the latter circumstances comes from studies of trihalides even further removed from zirconium, namely $RuBr_3$ and $MoBr_3$. Broderson et al.[21] first showed by single-crystal film techniques that $RuBr_3$ crystallizes in a larger ($Z = 4$) orthorhombic cell in space group *Pnmm* (nonstandard setting), the axes of which are related to those of the hexagonal cells discussed above as $a_O = a_H$, $b_O = \sqrt{3}b_H$, $c_O = c_H$. They observed 40% of the possible "fine-structure" reflections unique to the larger cell together with 76% of the 100-fold stronger reflections from the hexagonal pseudocell (which alone could be refined isotropically in $P6_3/mcm$ to $R = 7.1\%$). The orthorhombic solution contains chains of confacial octahedra as before, but the metals are now paired within the chains ($\Delta d \sim 0.4$ Å). Babel[22] later demonstrated that an apparently hexagonal $MoBr_3$ resulted from trilling (drilling) of the same orthorhombic cell about the common (nonstandard) c axis. This behavior was also shown to generate the reciprocal lattice for a hexagonal cell with doubled a and b axes that had been reported earlier.[17] The structure was approximated by refinement of just the observed reflections unique to the orthorhombic cell.

The availability of good single crystals of ZrI_3 from vapor-phase transport reactions that were not trilled (or twinned) prompted us to reexamine this structural question. Although data sets for both hexagonal and orthorhombic cells give what individually appear to be satisfactory refinements with paired metal atoms, the observation of many extra reflections unique to the orthorhombic cell (some by Guinier powder methods as well) leaves no doubt that the lower symmetry structure is correct. During this study we also learned that others have refined data from trilled crystals of ZrI_3 and several related examples in the orthorhombic cell.[23]

Experimental Section

Syntheses. The crystal of ZrI_3 used for the single-crystal studies was obtained from a reaction of ZrI_4 and Zr (powder) together with a small amount of AlI_3 to aid transport in a sealed tantalum tube at 800 °C. The crystals grow as well-faceted needles with the long direction parallel to the hexagonal c axis. They were generally black with a faint blue-green reflectance. Some crystals obtained by Daake[5] were also available. A single-phase sample near the upper limit, $ZrI_{3.4-3.5}$, was achieved by reaction of Zr and ZrI_4 (in proportions to give $ZrI_{3.50}$) at 800 °C for 10 days.

Crystallography. Hexagonal Cell. A set of data was collected in the hexagonal setting in order to judge better the nature of the solutions that could be obtained in the $P3$, $P321$, $P\bar{6}2m$, and $P6_3/mcm$ groups. A needlelike crystal of dimensions 0.1 × 0.1 × 0.45 mm that had been sealed under nitrogen within a 0.2-mm thin-walled capillary was used. A full sphere of reflection data was measured at room temperature to $2\theta = 50°$ on a Syntex $P2_1$ diffractometer with monochromatized Mo Kα radiation.

Solutions in six possible space groups, trigonal included, were consistent with the Patterson map and allow unequal Zr–Zr distances in this general structure type. Construction and refinement of the structure in $P3$ clearly showed unequal Zr–Zr distances (at 20σ). This result suggested that unequal metal spacings can be deduced even for an hexagonal setting and that this disposition was not the result of coupling between otherwise equivalent atoms. In addition, the y coordinates of both iodines refined to within 1σ of zero and the z coordinate of I2 to within 3σ of $^1/_2$ when the z for I1 was fixed at 0. The latter are all fixed parameters in higher symmetry space group choices. As a consequence, only $P321$, and $P\bar{6}2m$ needed further consideration. These are distinguished by the symmetry at iodine and the relationship between B_{13} and B_{23}. Refinement in $P321$ gave $B_{23} = 0.0$ within 1σ, which is the condition for $P\bar{6}2m$. The $P3$ refinement behaved similarly. Refinement in $P\bar{6}2m$ was uneventful, and both final F and ΔF maps showed nothing amiss. The zirconium occupancy refined to 0.99 (1), and the structure, to $R/R_w = 2.6/4.2\%$, GOF = 1.08, with the largest residual <0.4 e/Å.[3] The Zr–Zr distances differed by 27σ. Only four weak reflections out of 198 were $h0l$ with l odd, the condition required by $P6_3/mcm$.

Finally, we refined the same data, suitably averaged, in the published model ($P6_3/mcm$) with the equal Zr–Zr distances to give $R/R_w = 3.7/11.9\%$, GOF = 3.07 ($R_{av} = 0.024$). The thermal ellipsoids showed no anomalies (B_{33}/B_{11} (Zr) = 1.91). The iodine x coordinates scarcely differed from those just above (by 3.6σ), while the metal atoms were constrained to mirror planes midway between the iodine layers.

Orthorhombic Cell. The same crystal was then studied with the aid of oscillation, Weissenberg (Cu Kα), and precession (Mo Kα) methods. The needle (pseudohexagonal) axis was defined as $\bar{c}$ for this work. A 3-day exposure of a zero level ($hk0$) Weissenberg photograph showed a few weak reflections consistent with a primitive orthorhombic cell. Precession photographs of the $0kl$ and $1kl$ levels confirmed the primitive orthorhombic cell and yielded the $k + l = 2n$ condition for $0kl$ reflections. The corresponding "n" glide perpendicular to a is appropriate to only *Pnmm*. The unit cell parameters determined were about $a = 7.23$, $b = 12.48$, and $c = 6.69$ Å.

Three-dimensional diffraction data were obtained for the orthorhombic cell at 20 °C with the aid of a four-circle Rigaku AFC6R (rotating anode) diffractometer and graphite-monochromated Mo Kα radiation with the tube operating at a power 50 kV × 120 mA. Twenty-five reflections were readily indexed in the hexagonal setting, and long exposure of axial (Polaroid) photographs revealed no extra reflections. Some of the weak extra reflections that had been observed in the Weissenberg and precession photographs were then added, tuned, and refined to give an effectively orthorhombic cell with approximate lattice parameters $a = 7.293$ (4) Å, $b = 12.596$ (9) Å, $c = 6.686$ (3) Å, $\alpha = 89.95$ (5)°, $\beta = 90.02$ (4), and $\gamma = 89.92$ (5)°. [For comparison, constrained refinement of 25 Guinier powder pattern data from a different sample using Si as an internal standard gave $a = 7.292$ (2) Å, $b = 12.594$ (6) ($=\sqrt{3} \times 7.287$ (3)) Å and $c = 6.679$ (2) Å.]. Thirty-minute exposures of axial Polaroid photographs on the diffractometer confirmed the Laue symmetry *mmm* and the unit cell parameters. Diffraction data were measured for 2997 reflections in the octants $h,\pm k,l$ up to $2\theta = 70°$, giving 1446 observed data with $I/\sigma(I) \geq 3$. The crystal showed no decay according to 3 standard reflections measured every 100 reflections throughout the data collection.

The diffraction data exhibited the condition $k + l = 2n$ for $0kl$ reflections, indicating the probable space group *Pnmm*. They were transformed to the standard setting *Pmmn* (where the pseudohexagonal (needle) axis becomes b) and corrected for Lorentz and polarization effects and for absorption empirically by using the average of three azimuthal ψ scans. Refinements were carried out by full-matrix, least-squares methods using the TEXSAN version 2 structure solution package.[24] The scattering factor data therein include corrections for the real and imaginary parts of anomalous dispersion. Initial parameters for I1 and I2 were determined from a three-dimensional Patterson map, and these allowed the remaining atoms to be deduced from a Fourier difference map. Two cycles gave convergence with reasonable isotropic thermal parameters for all atoms. Refinement with anisotropic thermal parameters converged in three more cycles at $R = 0.022$ and $R_w = 0.042$. Inclusion of reflections with $I/\sigma(I) \geq 2$ gave $R = 0.026$ and $R_w = 0.046$, and all parameters stayed within 1σ. Refinement of all data on F gave

Table I. Crystal Data for ZrI_3[a]

space group;	*Pmmn*	T, °C	20
Z	(No. 59); 4	μ(Mo Kα), cm^{-1}	152.0
a, Å	12.594 (6)	transm factor: max–min	0.655–1.019
b, Å	6.679 (2)	R[b]	0.022
c, Å	7.292 (2)	R_w[c]	0.042
V, Å^3	613.4 (1)		

[a] Cell data from Guinier powder pattern with Si as an internal standard, $\lambda = 1.54056$ Å. [b] $R = \sum||F_o| - |F_c||/\sum|F_o|$. [c] $R_w = [\sum w(|F_o| - |F_c|)^2/\sum w(F_o)^2]^{1/2}$; $w = 1/\sigma^2(F)$.

(18) Babel, D.; Rüdorff, W. *Naturwissenschaften* **1964**, *51*, 85.
(19) Simon, A. Private communication, 1979.
(20) Lewis, J.; Machin, D. J.; Newnham, I. E.; Nyholm, R. S. *J. Chem. Soc.* **1962**, 2036.
(21) Brodersen, K.; Breitbach, H. K.; Thiele, G. *Z. Anorg. Allg. Chem.* **1968**, *357*, 162.
(22) Babel, D. *J. Solid State Chem.* **1972**, *4*, 410.
(23) Krebs, B. Private communication, 1986. Rüssman, U. Dissertation, Westfälische Wilhelms Universität, Münster, FRG, 1986.
(24) Molecular Structure Corp., College Station, TX.

Table II. Positional Parameters for ZrI_3

atom	type, sym[a]	x	y	z	B_{eq}, Å^2
I1	4f, *m*	0.08585 (5)	$-1/4$	0.58754 (9)	1.96 (3)
I2	4f, *m*	0.08872 (5)	$1/4$	0.91313 (9)	1.93 (3)
I3	2b, *mm*	$1/4$	$-1/4$	0.0807 (1)	1.95 (3)
I4	2a, *mm*	$1/4$	$1/4$	0.4299 (1)	1.86 (3)
Zr	4e, *m*	$1/4$	−0.0125 (1)	0.7521 (1)	1.54 (3)

[a] Space group *Pmmn*, origin at $\bar{1}$.

Table III. Interatomic Distances (Å) and Angles (deg) in ZrI_3

	Distances		
Zr–Zr	3.172 (2)	I2–Zr	2.929 (1)
Zr–Zr	3.507 (2)	I3–Zr	2.874 (1)
I1–Zr	2.868 (1)	I4–Zr	2.931 (1)
	Angles		
I1—Zr–I1	92.23 (4)	I2–Zr–I2	87.81 (4)
I1–Zr–I2	89.93 (3)	I2–Zr–I3	89.78 (3)
I1–Zr–I3	92.50 (2)	I2–Zr–I4	87.88 (3)
I1–Zr–I4	89.75 (3)	I3–Zr–I4	176.74 (3)

$R = 0.059$ and $R_w = 0.073$. Refinement of the four iodine atom occupancies (relative to Zr) with $3\sigma(I)$ data gave values that were not significantly different from unity, 1.006 (6), 1.004 (6), 1.008 (4), and 1.000 (4), respectively ($ZrI_{3.01(1)}$), so they were all set at 1.0. The final refinement included corrections for secondary extinction. The final ΔF map was featureless with a maximum of 1.4 e/Å^3 that was 0.63 Å from Zr together with a nearby minimum of −1.3 e/Å^3. Table I summarizes some crystal data. Large correlation effects precluded refinement in monoclinic space groups $P2_1/n$ or $P2/n$.

Results and Discussion

ZrI_3 Structure. The positional parameters for orthorhombic ZrI_3 and important distances and angles are given in Tables II and III. Additional information on data collection and refinement, the anisotropic displacement parameters, more distances and angles, and the structure factor data are available as supplementary material. A [101] view of two of the $^1_\infty[ZrI_{6/2}]$ chains that lie parallel to $\vec{b}$ is shown in Figure 1.

The structure of ZrI_3 consists of approximately hcp iodine atoms with the zirconium atoms bonded in every third string of antiprismatic sites that run normal to these, giving infinite chains of confacial ZrI_6 octahedra parallel to $\vec{b}$. However, this model is significantly distorted as the metal atoms bond in pairs, undergoing alternate displacements of 0.084 Å from the equally spaced positions of the ideal model to generate Zr–Zr distances of 3.172 (2) and 3.507 (2) Å. Mirror planes at $y = 1/4$ and $3/4$ contain all iodine atoms and bisect the long and short Zr–Zr separations. The iodine atoms respond to the metal displacements by moving outward from the metal axis where the Zr–Zr distance shortens (I1, I3, $\bar{d}$(I–I) = 4.144 Å) and inward where the opposite is true (I2, I4, $\bar{d}$ = 4.066 Å), whereas the I–I separations between these triangles average an intermediate 4.095 Å. The Zr–I distances are somewhat less within the Zr–Zr dimer (2.870 Å) than between them (2.930 Å), reflecting something of a matrix effect[25] from the iodine lattice. The chains pack such that the centers of the dimers alternate between $y = 1/4$ and $3/4$ in rows of chains centered in mirror planes at $x = 1/4$ and $3/4$ (Figure 1).

Two other zirconium iodides exhibit comparable Zr–Zr bonding. In $Cs_3Zr_2I_9$, Zr–Zr dimers with bond lengths of 3.13 Å occur in a defect hexagonal perovskite type of structure, basically within similar confacial octahedral chains of iodine in which just two-thirds of the sites contain zirconium.[26] In ZrI_2, zigzag chains of metal atoms run between nominally close-packed sheets of iodine such that Zr–Zr bonds form through shared edges of the octahedra.[27] These Zr–Zr distances are 3.185 Å, slightly greater than 3.172 Å in ZrI_3. The matrix effect of the approximately close-packed iodine atoms in limiting Zr–Zr bonding between (ZrI_6) units seems to be relatively fixed in the three examples.

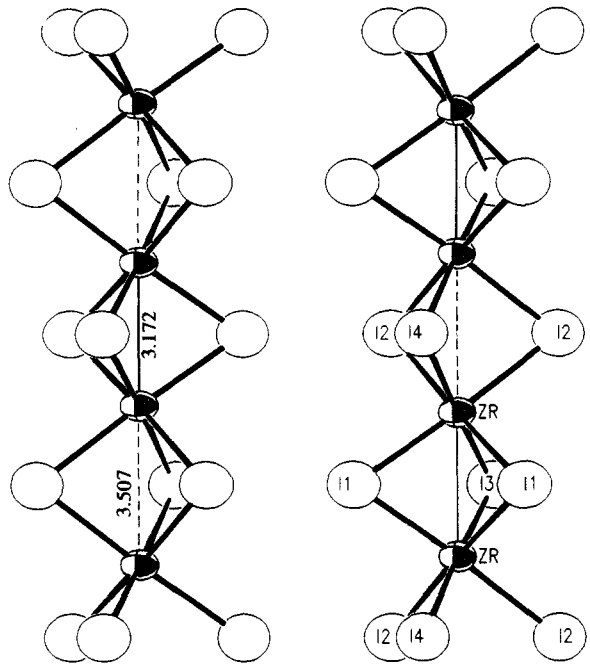

Figure 1. A [101] view of the cell in ZrI_3 (90% probability thermal ellipsoids), showing two of the semiinfinite chains that run parallel to $\vec{b}$. Mirror planes at $y = 1/4$ and $3/4$ bisect the long and short Zr–Zr distances.

Examples of chains analogous to those in ZrI_3 but with apparently equal metal–metal distances have been found in the isoelectronic M^ScX_3 (M = Cs, Rb; X = Cl, Br, I),[28] and more examples of both paired and equally spaced scandium chains will be forthcoming.[29]

This ZrI_3-type structure seems to provide a good choice when metal–metal bonding is important. An ideal close-packed halogen lattice allows metals centered in adjoining octahedral sites to approach distinctly (18%) closer through shared faces of the polyhedra than via shared edges, and this is the contrast between the (ideal) β-$TiCl_3$ and the BiI_3 types. This difference is also reflected in the low magnetic moments generally observed for those phases classified with the β-$TiCl_3$-type, etc. structure(s) versus the higher, even normal, values usually found for BiI_3-type phases near room temperature. (Distorted variations of the latter with more electrons, Nb_3X_8 for instance,[30] are an obvious exception.) It is therefore surprising that $TiCl_3$ and $TiBr_3$ occur in both the BiI_3 and the β-$TiCl_3$ (ZrI_3?) structure types. Metal–metal bonding in the ZrI_3-type chain structure should be stronger in the presence of the smaller halides, whereas such interactions in the BiI_3 arrangement without distortion are limited to the repeat length for bromide or chloride, $\geq \sim 3.4$ Å. It may be that participation of the halide in the metal–metal bonding interaction along the chains is more significant with iodide in TiI_3, ZrI_3, etc.

One problem remaining with this phase is its evident nonstoichiometry, ZrI_3–$ZrI_{3.4-3.5}$. Daake[5] found that the apparent hexagonal lattice constants a and c regularly decreased and increased, respectively, on oxidation, reasonable changes for the removal of Zr–Zr bonding, and extra lines appeared in the powder pattern in the process as well. Refinement of Guinier data for our $ZrI_{3.4-3.5}$ sample in the orthorhombic cell gave $a = 12.528$ (9) Å, $b = 6.6731$ (7) Å, and $c = 7.2382$ (8) Å. These are very close to the hexagonal equivalents obtained on a diffractometer by Wrazel[10] for a $ZrI_{3.40}$ crystal, and they differ only by 0.02 Å in c from those of Daake for an analyzed sample $ZrI_{3.43(5)}$. The structure of the $ZrI_{3.40}$ sample was refined in the high-symmetry hexagonal group with zirconium vacancies, i.e., $Zr_{0.881(4)}I_3$ (R/R_w = 5.9/9.1%). However, this is doubtlessly incorrect in detail; our

(25) Corbett, J. D. *J. Solid State Chem.* **1981**, *37*, 335.
(26) Guthrie, D. H.; Meyer, G.; Corbett, J. D. *Inorg. Chem.* **1981**, *20*, 1192.
(27) Corbett, J. D.; Guthrie, D. H. *Inorg. Chem.* **1982**, *21*, 1747.
(28) Meyer, G.; Corbett, J. D. *Inorg. Chem.* **1981**, *20*, 2627.
(29) Lachgar, A.; Corbett, J. D. Unpublished research.
(30) Simon, A.; von Schnering, H.-G. *J. Less-Common Met.* **1966**, *11*, 31.

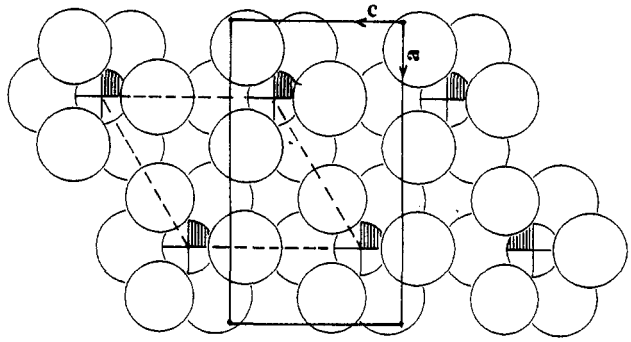

Figure 2. Interrelationship between the [001] projection of the hexagonal pseudocell and the [010] view of the larger orthorhombic cell (*Pmmn*) of ZrI_3. Both views are along the confacial chains and normal to the iodine layers.

Table IV. Contrasting Refinement Results for the Same ZrI_3 Crystal in Different Space Groups

	space group, lattice		
	$P6_3/mcm$, hexag	$P\bar{6}2m$, hexag	*Pmmn*, orthorh
2θ limit, deg (Mo Kα)	50	50	70
R/R_w, %	3.7/11.9	2.6/4.4	2.2/4.2
rflcns/params	112/8	198/13	741/28
d(Zr–Zr), Å	3.340 (1) × 2	3.245 (5), 3.434 (5)	3.172 (2), 3.507 (2)
$B_{\parallel}/B_{\perp}$ for Zr[a]	1.9	1.81	1.03

[a] The largest ratio of B_{ii} along and normal to the chain axis.

oxidized sample exhibited several extra lines in the Guinier pattern as well as distortions that could not be accounted for with the orthorhombic structure.

Other Refinements and Studies. It is very informative to compare the refinement results for ZrI_3 in the three space groups $P6_3/mcm$, $P\bar{6}2m$, and *Pmmn* as well as to consider inferences that may be drawn from other crystallographic studies and from theory. Figure 2 compares the [010] projection of the refined atom positions in orthorhombic ZrI_3 (origin at $\bar{1}$) with the [001] orientation of the related hexagonal cell. Both are normal to the iodine layers. Two other equivalent orientations of the orthorhombic cell are possible, each rotated by 120°, and these are presumably present in the trilled crystals noted by others. Fortunately, our crystals showed no evidence of this problem.

Table IV summarizes some of our results from the refinement of data from the same crystal in all three space groups that have been applied to this structure type (or types). These nicely illustrate some of the pitfalls that can be encountered with the utilization of only automatic search routines. Residuals for the two hexagonal solutions naturally ignore all of the weak reflections unique to the orthorhombic cell; they probably are also somewhat low in comparison because of the lower 2θ limit for the data. At face value, the R values for all three would probably be considered acceptable although the large value of R_w for the $P6_3/mcm$ solution (also obtained by others[10]) indicates that the weaker reflections are poorly accounted for by the model. Iodine scattering presumably dominates the strong reflections, so that this discrepancy must be, at least in part, a signal of poor zirconium parameters. Allowing the metals to move along $\vec{c}$ in $P\bar{6}2m$ solves the large R_w problem and properly produces unequal Zr–Zr distances (Δd = 0.19 Å), but the result is still wrong! Note that a substantial elongation of the zirconium thermal ellipsoid along the chain axis ($\vec{c}_H$) that ordinarily might be expected to manifest this error did not appear in either solution.

The correctness of the orthorhombic cell is established by the observation of 196 (out of a total of 741) reflections that are unique to the larger primitive orthorhombic cell, namely those for which $(h_O + l_O)/2 = h_H \neq n$ (in this orientation). These include the reflections that can be indexed with a hexagonal cell if the a and b axis lengths are (probably incorrectly) doubled,[22] as with TiI_3.[17] The strongest of the weak reflections unique to the orthorhombic cell is calculated to be only 0.20% of the most intense with Guinier polarization, and the strongest observed on the diffractometer is 0.90% of I(max) without any corrections. These would generally not be found by tuning search routines or seen in either axial Polaroid photos on the diffractometer or normal Debye–Scherrer patterns.

Four or five of these weak reflections can also be seen in an (Enraf-Nonius) Guinier photograph for a stoichiometric sample prepared by Daake [a = 12.594 (6) Å, b = 6.679 (2) Å, c = 7.292 (2) Å)]. These are probably the best cell parameters available for ZrI_3 because they are based on silicon as an internal standard, whereas parameters based on diffractometer measurements may involve appreciable systematic errors owing to imperfect alignment.[31] Earlier intercomparisons of ZrX_3 lattice constants[5,10] that had been obtained by the two different methods are therefore not apt to be very meaningful.

The $P\bar{6}2m$ space group suggested by Holze[4] on the basis of one observed (001) reflection for each of the zirconium and titanium trihalides (but not seen with a single crystal of TiI_3[17]) and the inferred importance of hexagonal 00l reflections with $l = 2n + 1$[6,10] do not seem appropriate to these zirconium problems. Guinier powder patterns calculated in $P\bar{6}2m$ for ZrI_3 and $ZrCl_3$ with the refined positional parameters (Table II) show that 00l reflections with $l \neq 2n$ are very weak indeed, ≤0.1% of I(max). The equivalent reflections are of course systematically absent with the symmetry of *Pmmn*. If reflections of this type are real (and they are in fact not regularly observed), then they must reflect an unappreciated and fairly rare structural variant.

A particularly reasonable aspect of this particular structure for $^1_\infty[MX_{6/3}]$ chains with metal pairing is that the inward and outward motions of bridging halides that surround the long and short M–M distances, respectively, can be better accommodated. The presence of an inversion center at $^1/_2, ^1/_2, ^1/_2$ relates Zr_2 dimers in two chains centered at $x = ^1/_4$ and $x = ^3/_4$ (Figure 2), while these must all be at the same height in $P\bar{6}2m$. In a larger view, the correct structure contains layers of chains normal to $\vec{a}$ that have alternate displacements. The consequent nesting appears very reasonable; all important interchain I–I distances fall in the range of 4.18–4.28 Å, while the intrachain values range between 4.06 and 4.15 Å (supplementary material).

Metal–Metal Bonding. The structure observed for ZrI_3 is obviously driven by the dimerization of the zirconium atoms, and the same probably applies to most other analogues as well judging from the similarity of properties. Although this distortion might be described as a Peierls type, the problem is not really one-dimensional. The halides defining the layers and the confacial octahedra provide a large part of the compounds' resistance to the dimerization, the so-called elastic energy of the crystal hosts. The smaller I–I distances about the long Zr–Zr separations, the 67° internal angles at iodine around the dimers, and shorter Zr–I distances therein are all manifestations of strong Zr–Zr bonding in an iodine matrix. Similar factors have been noted to pertain to analogous $M_2X_9^{3-}$ examples.[26] We earlier speculated that the structural choices made by the titanium halides suggest that stronger metal–metal bonding occurs with the iodide, in spite of its greater size. Perhaps this occurs because greater covalency both leads to more mixing in the bonding state and decreases unfavorable Madelung energy terms that arise during the distortion. There is some evidence to suggest that the same trend may apply to the zirconium trihalides, as follows.

An important aspect of these structural problems is the recognition that the metal–metal bonding and the degree of distortion from the high-symmetry β-$TiCl_3$ structure in these examples can be a continuous function of temperature as well as dependent on halide, metal, composition, pressure, etc. This is because not only does the parent space group $P6_3/mcm$ bear a group–subgroup relationship to the much more suitable orthorhombic *Pmnn* but this pair also fulfills all criteria of Landau theory for them to be related to a second-order phase transition.[32] The appearance of

(31) Jones, P. G. *Chem. Soc. Rev.* **1984**, 157.
(32) Franzen, H. F. *J. Solid State Chem.* **1990**, *85*, 173.

trilled crystals in other work is a strong indication that those particular samples were synthesized at a temperature near or above that for the onset of distortion from the hexagonal model with equally spaced metal atoms.

We further note that the results of refinement of $ZrCl_3$ in $P6_3/mcm$[10] suggest appreciably less distortion is present in that phase at room temperature than in the iodide. The smaller halide means zirconium–zirconium bonding is already significantly greater in the idealized $ZrCl_3$, 3.067 Å to two neighbors (total Zr–Zr bond order $n = 0.565$) relative to a 3.34-Å separation in the hypothetical ZrI_3 analogue ($n = 0.20$) and 3.172 Å to only one neighbor in the real iodide ($n = 0.38$ if the long separation is taken as nonbonding). The relative X-ray scattering by zirconium is significantly more important in the chloride than in the iodide, and yet the forced high-symmetry refinement of $ZrCl_3$ still gave fairly good R/R_w values, 3.0/4.4%, from a relatively large set of reflection data.[10] Recall that two studies of the iodide gave much more disparate residuals, 6.0/10.4%[10] and 3.7/11.9% (Table IV), appropriate to the dominance of iodine scattering. The temperature dependencies of the distortions in all of these structures should be interesting.

Other properties of most of these trihalides have not been well investigated. However, preliminary conductance and magnetic susceptibility data for the three ZrX_3 phases are certainly consistent with a metal-paired structure. Single-crystal conductivities at room temperature range between 2×10^{-5} ($ZrCl_3$) and 2×10^{-4} (ZrI_3) Ω^{-1} cm^{-1}, which are fairly comparable to values of 1×10^{-7} and 2.5×10^{-3} Ω^{-1} cm^{-1} for the corresponding NbX_4 phases where similar paired chains form via metal–metal bonding through shared edges of distorted halide octahedra. A strong localization of bonding electrons is implied for all. Magnetic data for the three zirconium halides[13,33] appear qualitatively consistent with the structural model after the effects of appreciable field-dependent impurities are removed; these all show a small paramagnetism that with decreasing temperature first increases slightly to moderately and then falls off markedly. The susceptibility of HfI_3 is also low and nearly temperature-independent down to 80 K.[16] The likely temperature dependencies of the metal–metal distances and thence of the energy gaps that pertain to both the conduction and the magnetic properties will obviously complicate analyses of the data.

Acknowledgment. Professor B. Krebs is thanked for discussions and the communication of unpublished structural results on several trihalides of this type during our investigations. Professor H. F. Franzen also provided helpful information and advice. This research was supported by the National Science Foundation, Solid State Chemistry, via Grants DMR-8318616 and -8902954 and was carried out in facilities of the Ames Laboratory, DOE.

Registry No. ZrI_3, 13779-87-8.

Supplementary Material Available: Tables of data collection and refinement information, distances, angles, and anisotropic thermal parameters for orthorhombic ZrI_3 (3 pages); a listing of F_o and F_c for the same structure (6 pages). Ordering information is given on any current masthead page.

(33) Baker, W. A.; Janus, A. R. *J. Inorg. Nucl. Chem.* **1964**, *26*, 2087.

Contribution from the Department of Chemistry,
Iowa State University, Ames, Iowa 50011

Encapsulation of the Platinum and Neighboring Metals within Cluster Iodides of Rare-Earth Elements

Martin W. Payne and John D. Corbett*

Received September 21, 1989

Syntheses of new cluster phases containing encapsulated heterometals have been explored through reactions between the rare-earth metal Y, Pr, or Gd (R), RI_3, and a 3d, 4d, or 5d element (Z) at 750–1000 °C in sealed Nb containers. New $Pr_7I_{12}Z$ ($Sc_7Cl_{12}N$-type) phases are obtained for Z = Cu, Ru, Rh, Pd, Re, Os, Ir, and Pt. New $Gd_7I_{12}Z$ phases occur for Z = Ni, Cu, Ru, Rh, Pd, Os, Ir, Pt, and Au. In contrast, new $Y_6I_{10}Z$ analogues of the previously reported $Y_6I_{10}Ru$ occur with Z = Co, Ni, Rh, Os, Ir, and Pt and as $Pr_6I_{10}Os$. The structures of $Y_6I_{10}Os$ and $Y_6I_{10}Ir$ have been refined for comparison with $Y_6I_{10}Ru$ ($P\bar{1}$, $Z = 1$; $a = 7.6268$ (8), 7.6154 (7) Å, $b = 9.518$ (1), 9.535 (1) Å, $c = 9.617$ (1), 9.577 (1) Å, $\alpha = 107.72$ (1), 107.67 (1)°, $\beta = 97.17$ (1), 97.11 (1)°, $\gamma = 105.13$ (1), 105.15 (1)°; $R/R_w = 3.1/4.2$, 3.7/4.3%, respectively). The sizable tetragonal compression observed earlier in the $Y_6I_{10}Ru$ cluster and thought to be electronically driven is only 44% as great in the isoelectronic Os phase and is virtually absent in $Y_6I_{10}Ir$. Relativistic effects may be important in the bonding of the 5d interstitials. Unsuccessful syntheses, orbital populations in the various clusters, volume changes seen among the $R_7I_{12}Z$ phases, and matrix effects in intercluster bonding are also discussed and interrelated.

Introduction

Exploratory synthesis can in the best of times provide a continuing series of surprises. For instance, once the concept was clear that interstitial atoms (Z) afforded new cluster[1] and condensed cluster[2,3] halides of the early transition metals, a large and diverse family of zirconium cluster chloride stoichiometries and structures were synthesized. These were all based on $Zr_6Cl_{12}Z$ units in which one of a relatively small group of atoms was bonded, H or Be–N.[4,5] Use of the iodides instead gave $Zr_6I_{12}Z$-type cluster phases that also encapsulated heavier main-group elements, Al, Si, Ge, or P.[6,7] Shortly later, 3d metals were found to bind within zirconium clusters, first for Cr–Co in iodides[8] and later for Mn–Ni in the chlorides.[9] Most of these examples can be interpreted fairly well with the aid of simple extended Hückel calculations and in

(1) Smith, J. D.; Corbett, J. D. *J. Am. Chem. Soc.* **1985**, *107*, 5704.
(2) Ford, J. E.; Corbett, J. D.; Hwu, S.-J. *Inorg. Chem.* **1983**, *22*, 2789.
(3) Hwu, S.-J.; Corbett, J. D.; Poeppelmeier, K. R. *J. Solid State Chem.* **1985**, *57*, 43.
(4) Ziebarth, R. P.; Corbett, J. D. *J. Am. Chem. Soc.* **1989**, *111*, 3272 and references therein.
(5) Ziebarth, R. P.; Corbett, J. D. *Acc. Chem. Res.* **1989**, *22*, 256.
(6) Smith, J. D.; Corbett, J. D. *J. Am. Chem. Soc.* **1986**, *108*, 1927.
(7) Rosenthal, G.; Corbett, J. D. *Inorg. Chem.* **1988**, *27*, 53.
(8) Hughbanks, T.; Rosenthal, G.; Corbett, J. D. *J. Am. Chem. Soc.* **1988**, *110*, 1511.
(9) (a) Rogel, F.; Zhang, J.; Payne, M. w.; Corbett, J. D. *Adv. Chem. Ser.* **1990**, *No. 226*, 369. (b) Zhang, J.; Corbett, J. D. Unpublished research.

0020-1669/90/1329-2246$02.50/0